Journal of Materials Chemistry

Dynamic Article Links

Cite this: *J. Mater. Chem.*, 2012, **22**, 15495

www.rsc.org/materials

COMMUNICATION

Functionalization of silver nanowire surfaces with copper oxide for surface-enhanced Raman spectroscopic bio-sensing†

Peng Peng,*[ab] Hong Huang,[a] Anming Hu,[a] Adrian P. Gerlich[a] and Y. Norman Zhou*[ab]

Received 18th May 2012, Accepted 21st June 2012
DOI: 10.1039/c2jm33158f

A facile method to fabricate copper oxide functionalized silver nanowires with high sensitivity to biomolecules is reported for the first time. The enhanced surface roughness of silver nanowire and the molecule capture capability of copper oxide nanoparticles account for the high sensitivity of this nanocomposite.

Noble metallic nanomaterials with different shapes and sizes have led to a variety of research fields including engineered nanodevices,[1,2] nanomedicine,[3,4] nanophotonics[5] and ultrasensitive sensing.[6] One-dimensional nanowires, particularly silver nanowires (Ag NWs), have attracted a great deal of interest with applications with their unique electrical and plasmonic properties.[7–12] For example, Garnett *et al.*[12] recently reported an approach for welding of Ag NWs by light introduced surface plasmon. The small gaps that form naturally at Ag NW junctions can concentrate light and generate an enhanced electromagnetic field which is a widely recognized phenomenon at the surface of noble metals. These areas, also called "hot spots", are usually found in between adjacent metal nanostructures if they are located sufficiently close to each other, *i.e.*, on the order of a few nanometers. Ag NW clusters with different gaps produced in the form of a thin film will more readily form a series of these "hot spots" compared with a consolidation of nanoparticles, which have been carefully deposited on the substrates with controlled gaps.

The generation of the surface plasmons has also been used to explain the increased electromagnetic fields formed on silver and gold surfaces which facilitate surface enhanced Raman scattering (SERS).[13,14] During Raman spectroscopy of biological samples, the use of visible lasers usually results in low intensity Raman scattering signals, and consequently there is motivation for developing detectors with increased sensitivity for such applications. SERS has been demonstrated as a powerful analysis technique for detecting trace amounts of targeted molecules[15–18] when these are adsorbed onto and between adjacent Ag NW surfaces where "hot spot" regions form near the intersecting nanowires. If a target molecule is located inside this hot spot within the laser footprint, the increased Raman signal allows one to more easily identify chemical species.[19,20] Zhang and co-workers[21] have shown that hot spots account for a disproportionately large contribution to the enhanced Raman signal[22,23] and this is considered a reliable and robust sensing technology in terms of both chemical and biochemical applications.[22,24,25] This has been examined for the food industry and diagnosis of diseases including cystic fibrosis[26] and diabetes mellitus.[27] However, many biomolecules (especially glucose) are difficult to detect by SERS due to a small normal Raman cross-section and poor or negligible adsorption on the bare silver surface.[28]

Nano-sized biomolecules[29] exhibit a fundamental feature of specific and strong complementary recognition interactions and several binding sites, which can interact with nanomaterials, particularly transition-metal oxides[30,31] through physical adsorption, electrostatic binding, specific recognition, and covalent coupling.[27,32–34] Copper oxide (CuO), is one such oxide that has gained increasing attention for sensor applications[35,36] because of its semiconducting nature and distinctive properties.[37–39] Integrating the high surface area and "hot spot" features resulting from the one dimensionality and plasmonic properties of Ag NWs with the high adsorption and preferential binding for biomolecules of CuO would combine the unique properties of both materials and lead to novel applications.

In this study, a facile approach to functionalize Ag NW clusters with CuO nanoparticles is examined for the first time. The high sensitivity of these composite nanomaterials for non-enzymatic bio-sensing applications has been demonstrated using D-glucose and adenine molecules *via* SERS technology.

Ag NWs were prepared in a polyol solution using a method modified from the literature.[40,41] Ag NWs were washed in deionized (DI) water to remove the ethylene glycol and PVP and condensed by centrifugation. Copper substrates were ultrasonically cleaned with acetone and diluted HNO_3. 50 μL Ag NW paste with 0.6 mole L^{-1} concentration was homogeneously coated on a 1 cm^2 area of copper substrate and dried at room temperature. Here, the copper substrate worked as a copper source to provide copper ions. After drying, the 1 cm^2 Ag NW films on the copper substrate were exposed to 0 μL, 50 μL, 100 μL, 150 μL and 500 μL distilled water from a dropper to grow CuO, and were labelled as A1, A2, A3, A4 and A5, respectively. For comparison, Ag NW films on cleaned glass without copper substrate were coated using same method and designated as sample A0.

[a]*Centre for Advanced Materials Joining, Department of Mechanical and Mechatronics Engineering, University of Waterloo, 200 University Avenue West, Waterloo, ON, N2L 3G1, Canada. E-mail: p5peng@uwaterloo.ca; nzhou@uwaterloo.ca*
[b]*Waterloo Institute for Nanotechnology, University of Waterloo, 200 University Avenue West, Waterloo, ON, N2L 3G1, Canada*

† Electronic supplementary information (ESI) available: Synthesis of Ag NWs and functionalization of Ag NW with CuO NPs, characterization of materials, calculation of average coverage and exposed interfacial area, EDS results of CuO NP and Raman spectra of substrates. See DOI: 10.1039/c2jm33158f

Cu oxidation would take place when the Ag NW and Cu were exposed to water in open air due to the different chemical potentials of Cu and Ag.[42–44] The following equations show the reactions.

$$Cu + O_2 \rightarrow Cu_2O \quad (1)$$

$$Cu_2O + O_2 \rightarrow CuO \quad (2)$$

The initially pristine Ag NWs deposited on a clean glass substrate were crosslinked randomly and formed clusters as depicted in Fig. 1a. The surface of Ag NWs which were deposited on a copper substrate started to nucleate and grow nanoparticles with more nanoparticles being decorated on the Ag NW surfaces with increasing volumes of water. After continually dropping 500 μL H_2O on 1 cm^2 Ag NW thin film on Cu substrate, the Ag surfaces were all covered by nanoparticles as illustrated in Fig. 1b. Fig. 1c clearly illustrates the increase of coverage of CuO particles on the individual Ag NW in samples A0 through A5. The nanoparticle diameters were in the range 5–10 nm and consisted of mainly CuO according to the XRD results (PDF, 89–2531 (ref. 45)), although they could not be detected in samples Al and A2 because of their low volume fractions, see Fig. 1d. The CuO particles on the surface of the synthesized sample A3 did not grow on the Ag NW surfaces until water was reintroduced, and they remained stable when kept in dry air. In order to understand the growth of CuO on Ag NW, TEM was employed to observe the Ag NW–Cu substrate interface on the thin sections cut by ultramicrotome. Fig. 2a illustrates the CuO nanocubes on the surface of a Ag NW. The inset image of Fig. 2b indicates that CuO grew on both the Cu substrate and Ag NW. The high resolution TEM image of the square area displays the CuO–Ag interface. According to the measurement of lattice fringes, the (111) plane is depicted on the Ag side (with a spacing of 2.31 Å), which is very close to 2.29 Å corresponding to the (200) plane in the CuO on the opposite side.[46] EDX confirmed that the nanoparticle consisted of only Cu and O in Fig. S1.† Due to the close lattice matching of these two planes in these materials, it appears there is an orientation relationship between Ag and CuO which is developed during oxide growth on the surface of the Ag NW. Therefore, it is suggested that the Cu atoms were oxidized first because of the different electrochemical potentials of Cu and Ag. Due

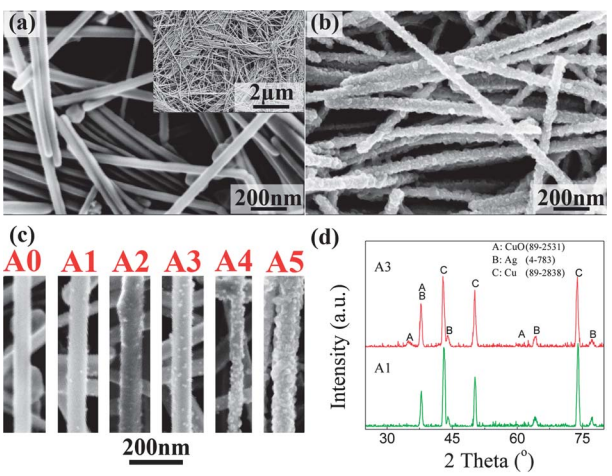

Fig. 1 SEM images of (a) Ag NW film in A0 (inset is low magnification image), (b) all covered Ag NW by NPs of A5. (c) Individual Ag NW of A0–A5. (d) X-ray diffraction spectra of A1 and A3.

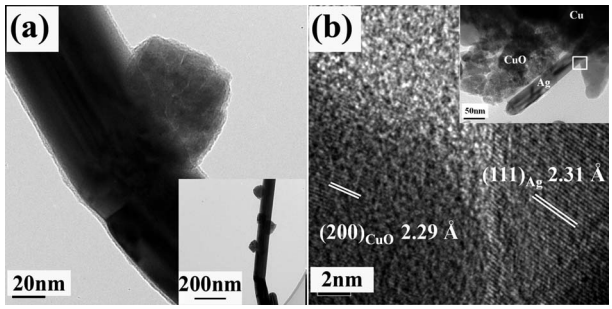

Fig. 2 TEM images of Ag NWs functionalized with CuO nanoparticles. (a) CuO nanoparticles decorated Ag NW. (b) CuO–Ag interface.

to the presence of water, Cu^+ ions are transported around the Ag NWs. When Cu^+ ions reach interfaces containing defects or high surface energies, for example the bare Ag atoms where the PVP coating is removed by the washing process, they may be reduced and combine with O ions to nucleate and form Cu_2O. Then, Cu_2O may be further oxidized to CuO and grow into cubic shapes as we observed. By changing the contact time of Ag NW/Cu with water, the amount of CuO, or rate of coverage, on Ag NW surfaces could be controlled.

If one assumes CuO to be a cube-shaped nanoparticle (as observed in Fig. 2a) the calculated average coverage of CuO particles on the surface (CuO–Ag contact area divided by Ag NW surface area) and the exposed interfacial area between CuO and the Ag nanowires (perimeter area of CuO divided by Ag NW surface area) for each sample are shown in Fig. 3a. A more detailed calculation was described in ESI Fig. S2.† Here, sample A3 corresponded to 8% and

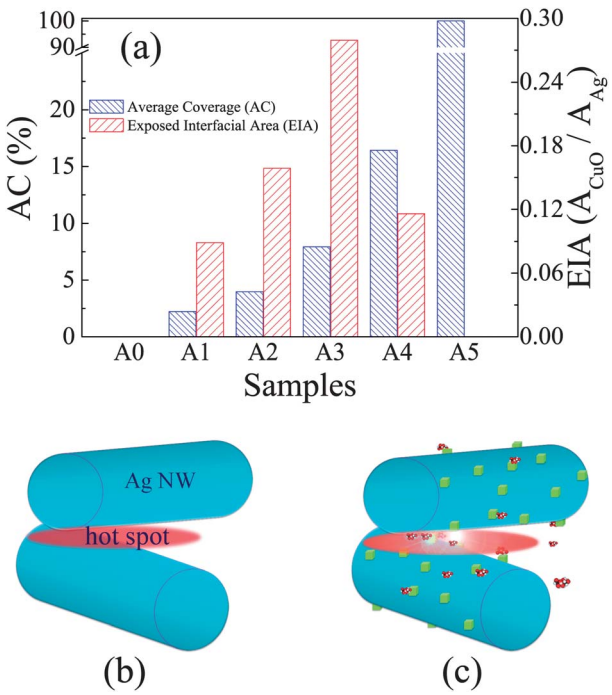

Fig. 3 (a) Calculated average coverage ($AC = A_{CuO–Ag\ contact}/A_{Ag}$) and exposed interfacial area ($EIA = A_{CuO\ perimeter}/A_{Ag}$) of CuO on Ag surface. Schematic illustrating of (b) "hot spot" in Ag NW junction and (c) CuO molecule physisorption sites on Ag surface for SERS sensing (cubes: CuO NPs, molecules: glucose).

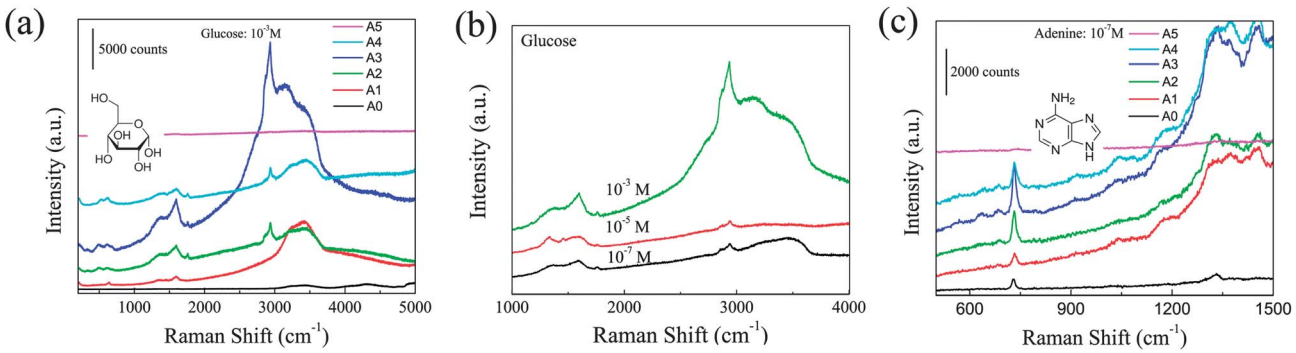

Fig. 4 SERS spectra of (a) D-glucose molecules with a concentration of 10^{-3} M obtained from the films of samples A0–A5 and a film formed by Ag NWs. (b) SERS spectra of D-glucose molecules with different concentrations 10^{-3} M, 10^{-5} M and 10^{-7} M obtained from A3. (c) SERS spectra of adenine molecules with a concentration of 10^{-7} M.

0.28 nm^2 of CuO perimeter area per nm^2 of covered silver surface (average coverage and exposed interfacial area of CuO on the Ag NW surface). Though some molecules, such as glucose mentioned previously, are extremely difficult to detect by SERS due to weak adsorption on the silver surface, this molecule easily attaches on CuO surfaces as demonstrated by electrochemical sensing.[34,47] The integration of these materials can combine the advantages of CuO NPs and Ag NWs for detection using the SERS technique. This provides a solution to enhance the adsorption of glucose on Ag surface, by introducing CuO as the physisorption positions of the molecules on Ag surface. For the CuO nanoparticles, the effective adsorption area for SERS is the area located in the enhanced electromagnetic field very close to Ag surface. In this case, it was evaluated by exposed interfacial area (perimeter area close to Ag) of CuO on Ag surface as indicated in Fig. 3a. Those CuO surfaces away from Ag surface do not appear to be contributing to the enhancement. The CuO sites preferentially capture glucose molecules on the Ag surface, and in particular the hot spots of intersecting Ag NWs, promoting high-efficiency SERS detection[48] as schematically illustrated in Fig. 3b and c. Furthermore, by functionalizing Ag NWs with CuO NPs, the roughness of Ag NW surface is increased which provides a higher area to adsorb molecules.[49]

To investigate the performance regarding electromagnetic enhancement of these CuO functionalized Ag NW films, D-glucose was adopted to evaluate the sensitivity of functionalized Ag NWs by SERS. Fig. 4a shows the Raman spectra of D-glucose molecules at a concentration of 10^{-3} M, a desired concentration for medical applications.[28] The highest sensitivity of D-glucose was exhibited using sample A3 (Fig. S3† indicates the results on glass and bare copper substrates). Two significant enhanced peaks were detected at 1597 cm^{-1} and 2938 cm^{-1}. Usually, the C–H stretching region located between 3000 and 2800 cm^{-1} tends to be broad and very difficult to be revealed using SERS. Here, the sharp C–H vibrational band has been successfully observed and exhibited a high intensity in the presence of 10^{-3} M D-glucose concentration, which represents a 200-fold increase in sensitivity compared with the SERS response of 10^{-2} M glucose using roughened Ag substrate and Ag colloid.[50] The functionalized Ag NWs with CuO presented sensitivity to low concentrated glucose molecules as well, see Fig. 4b. The enhancement reduced as the concentration decreased from 10^{-3} to 10^{-7} M but the peak at 2938 cm^{-1} was still visible. Though many reports developed glucose sensors using electrochemical methods, an enzyme was generally employed to improve the sensitivity.[51–53] Here, by combining this nanocomposite and SERS, glucose can be sensed without an enzyme at very low concentrations. Another molecule, adenine, a well characterized chemical component of DNA and RNA, was employed for SERS spectroscopic measurements. Fig. 4c shows the Raman spectra of adenine molecules at a concentration of 10^{-7} M. Samples A1–A4 displayed the characteristic peak at 732 cm^{-1} with high Raman scattering cross-section, similar to prior reported results,[21,54,55] and exhibited repeatable high SERS sensitivity. It also shows enhanced sensitivity compared with SERS of 8×10^{-5} M adenine using Ag NPs as previously reported by Kneipp *et al.*[56] Even without CuO nanoparticles, the Ag NW film A0 exhibits some sensitivity to adenine molecules due to the "hot spots" formed by intersecting nanowires as shown in Fig. 3b, and the sensitivity is dramatically increased when these are functionalized with CuO on the surface due to the effects of increased surface roughness adsorbance[38] as shown with samples A1–A3. However, as the surfaces of the Ag NWs became covered by more CuO in sample A4, the decreased exposed interfacial area of CuO on Ag suppressed the characteristic peak, see Fig. 5a. The enhancement would drop further if the entire surface of the Ag NW was covered by CuO and no exposed perimeter interface of CuO–Ag left as in sample A5. Consequently it appears that only the CuO–Ag interface is active in enhancing the Raman output, given that the nanowires completely covered CuO (sample A5) does not elicit any output whatsoever (see Fig. 1c and 5a). The intensities of Raman spectra for all samples at characterized peaks reproduced in Fig. 5a clearly indicated the enhancement using functionalized Ag NWs, where sample A3 exhibited the best sensitivity to both adenine and glucose molecules with 8% average coverage and 0.28 nm^2

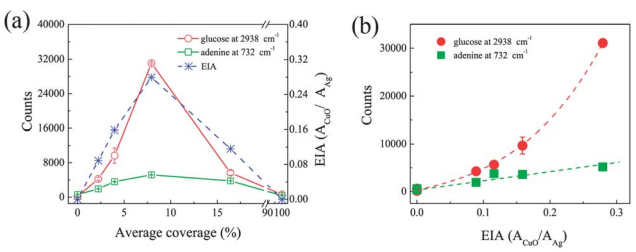

Fig. 5 (a) The intensities of characterized peaks for two molecules as functions of calculated average coverage of CuO on Ag NW surface. The exposed interfacial area of CuO *vs.* average coverage was plotted. (b) The intensities of characterized peaks as functions of the exposed interfacial area (EIA) of CuO.

exposed interfacial area of CuO on per nm^2 Ag NW surface. The magnitude of enhancement for detection of glucose was 200 times larger than that of pure Ag NWs. Fig. 5b indicates the relationship between enhancement of the detection of molecules and exposed interfacial area. A remarkable exponential relationship was found between sensitivity to detection glucose with exposed interfacial area, while a linear relation is observed for adenine. In the case of glucose, the enhancement may be dominated by the strong adsorption molecules on the exposed interfacial area. However, since there is no evidence for adenine adsorption on CuO, the enhancement for adenine may be solely due to the increased surface roughness when CuO NPs are introduced on Ag surface. Although glucose and adenine have very different groups and structures as shown in the inset structure formulae of Fig. 4a and c, the composite exhibited an exceptional increase in sensitivity compared with pure Ag NWs. It demonstrates that the Ag NW surface functionalized with CuO nanoparticles is a promising bio-sensitive material for many other different molecules as well, with further applications for bio-sensing with high sensitivity using SERS.

For the first time, it has been demonstrated that CuO can be grown on the surface of Ag NWs by changing the contact time of Ag NWs on a Cu substrate immersed in water. This facile approach allows controllable growth and adjusting the coverage of CuO on Ag NW. Due to the enhanced surface roughness and molecule capture capability of CuO nanoparticles functionalized Ag NWs, the nanocomposite showed high sensitivity to D-glucose and adenine molecules using SERS. This indicates that it is a promising material for bio-chemical sensor and other applications. The hybridization of these two kinds of unique materials with the facile method has potential for other practical applications and opens doors for other exciting new applications combining the advantageous properties of both materials.

Acknowledgements

Support from the Canadian Research Chairs (CRC) program, the State Scholarship Fund of China (no. 2010640009) and National Sciences and Engineering Research Council (NSERC) is greatly acknowledged. We are grateful for the comments and suggestions of Dr Xiaogang Li and Lei Liu from the Centre for Advanced Materials Joining at the University of Waterloo, and thank Mr Fred Pearson from Canadian Center for Electron Microscopy, McMaster University for help with TEM observation.

Notes and references

1 N. Chandrasekharan and P. V. Kamat, *Nano Lett.*, 2001, **1**, 67–70.
2 X. Xiong, A. Busnaina, S. Selvarasah, S. Somu, M. Wei, J. Mead, L. Chen, J. C. Aceros, P. Makaram and M. R. Dokmeci, *Appl. Phys. Lett.*, 2007, **91**, 063101.
3 E. C. Dreaden, M. A. Mackey, X. H. Huang, B. Kang and M. A. El-Sayed, *Chem. Soc. Rev.*, 2011, **40**, 3391–3404.
4 C. M. Cobley, J. Chen, E. C. Cho, L. V. Wang and Y. Xia, *Chem. Soc. Rev.*, 2011, **40**, 44–56.
5 J. A. Schuller, E. S. Barnard, W. Cai, Y. C. Jun, J. S. White and M. L. Brongersma, *Nat. Mater.*, 2010, **9**, 193–204.
6 J. N. Anker, W. P. Hall, O. Lyandres, N. C. Shan, J. Zhao and R. P. Van Duyne, *Nat. Mater.*, 2008, **7**, 442–453.
7 Y. Zhang and H. Dai, *Appl. Phys. Lett.*, 2000, **77**, 3015–3017.
8 T. Tokuno, M. Nogi, M. Karakawa, J. Jiu, T. T. Nge, Y. Aso and K. Suganuma, *Nano Res.*, 2011, **4**, 1215–1222.
9 L. Hu, H. S. Kim, J. Y. Lee, P. Peumans and Y. Cui, *ACS Nano*, 2010, **4**, 2955–2963.
10 L. Hu, J. W. Choi, Y. Yang, S. Jeong, F. L. Mantia, L. F. Cui and Y. Cui, *Proc. Natl. Acad. Sci. U. S. A.*, 2009, **106**, 21490–21494.
11 A. R. Madaria, A. Kumar, F. N. Ishikawa and C. Zhou, *Nano Res.*, 2010, **3**, 564–573.
12 E. C. Garnett, W. Cai, J. J. Cha, F. Mahmood, S. T. Connor, M. G. Christoforo, Y. Cui, M. D. McGehee and M. L. Brongersma, *Nat. Mater.*, 2012, **11**, 241–249.
13 M. Zhang, A. Zhao, H. Sun, H. Guo, D. Wang, D. Li, Z. Gan and W. Tao, *J. Mater. Chem.*, 2011, **21**, 18817–18824.
14 C. Zhu, G. Meng, Q. Huang, Z. Zhang, Q. Xu, G. Liu, Z. Huang and Z. Chu, *Chem. Commun.*, 2011, **47**, 2709–2711.
15 H. He, X. Xu, H. Wu and Y. Jin, *Adv. Mater.*, 2012, **24**, 1736–1740.
16 J. Yang, Z. Wang, X. Tan, J. Li, C. Song, R. Zhang and Y. Cui, *Nanotechnology*, 2010, **21**, 345101.
17 A. Hu and W. W. Duley, *Chem. Phys. Lett.*, 2008, **450**, 375–378.
18 A. J. Chung, Y. S. Huh and D. Erickson, *Nanoscale*, 2011, **3**, 2903–2908.
19 Y. Hang, Z. Y. Li, K. Yamaguchi, M. Tanemura, Z. Huang, D. Jiang, Y. Chen, F. Zhou and M. Nogami, *Nanoscale*, 2012, **4**, 2663–2669.
20 R. Kattumenu, C. H. Lee, L. Tian, M. E. McConney and S. Singamaneni, *J. Mater. Chem.*, 2011, **21**, 15218–15223.
21 X. Y. Zhang, A. Hu, T. Zhang, W. Lei, X. J. Xue, Y. Zhou and W. W. Duley, *ACS Nano*, 2011, **5**, 9082–9092.
22 M. S. Schmidt, J. Hübner and A. Boisen, *Adv. Mater.*, 2012, **24**, OP11–OP18.
23 Y. Fang, N. H. Seong and D. D. Dlott, *Science*, 2008, **321**, 388–392.
24 S. S. R. Dasary, A. K. Singh, D. Senapati, H. Yu and P. C. Ray, *J. Am. Chem. Soc.*, 2009, **131**, 13806–13812.
25 Y. He, S. Su, T. Xu, Y. Zhong, J. A. Zapien, J. Li, C. Fan and S. T. Lee, *Nano Today*, 2011, **6**, 122–130.
26 R. C. Stern, *N. Engl. J. Med.*, 1997, **336**, 487–491.
27 M. U. A. Prathap, B. Kaur and R. Srivastava, *J. Colloid Interface Sci.*, 2012, **370**, 144–154.
28 K. E. Shafer-Peltier, C. L. Haynes, M. R. Glucksberg and R. P. Van Duyne, *J. Am. Chem. Soc.*, 2003, **125**, 588–593.
29 G. J. Lee, S. I. Shin and S. G. Oh, *Chem. Lett.*, 2004, **33**, 118–119.
30 X. Xie, Y. Li, Z. Q. Liu, M. Haruta and W. Shen, *Nature*, 2009, **458**, 746–749.
31 G. Wang, X. Lu, T. Zhai, Y. Ling, H. Yang, Y. Tong and Y. Li, *Nanoscale*, 2012, **4**, 3123–3127.
32 L. Rocks, K. Faulds and D. Graham, *Chem. Commun.*, 2011, **47**, 4415–4417.
33 E. Katz and I. Willner, *Angew. Chem., Int. Ed.*, 2004, **43**, 6042–6108.
34 M. Shi, H. S. Kwon, Z. Peng, A. Elder and H. Yang, *ACS Nano*, 2012, **6**, 2157–2164.
35 J. Y. Li, S. L. Xiong, B. J. Xi, X. G. Li and Y. T. Qian, *Cryst. Growth Des.*, 2009, **9**, 4108–4115.
36 X. Zhang, G. Wang, X. Liu, J. Wu, M. Li, J. Gu, H. Liu and B. Fang, *J. Phys. Chem. C*, 2008, **112**, 16845–16849.
37 L. C. Jiang and W. D. Zhang, *Biosens. Bioelectron.*, 2010, **25**, 1402–1407.
38 S. Park, H. Boo and T. D. Chung, *Anal. Chim. Acta*, 2006, **556**, 46–57.
39 M. M. Rahman, A. J. S. Ahammad, J. H. Jin, S. J. Ahn and J. J. Lee, *Sensors*, 2010, **10**, 4855–4886.
40 Y. Sun, B. Gates, B. Mayers and Y. Xia, *Nano Lett.*, 2002, **2**, 165–168.
41 Y. Sun and Y. Xia, *Adv. Mater.*, 2002, **14**, 833–837.
42 P. L. Williams, Y. Mishin and J. C. Hamilton, *Modell. Simul. Mater. Sci. Eng.*, 2006, **14**, 817–833.
43 A. J. Bard, R. Parsons and J. Jordan, *Standard Potentials in Aqueous Solutions*, Marcel Dekker, New York, 1985.
44 P. Vanýsek, Electrochemical Series, in *Handbook of Chemistry and Physics*, Chemical Rubber Company, 88th edn, 2007.
45 O. García-Martínez, R. M. Rojas, E. Vila and J. L. Martín de Vidales, *Solid State Ionics*, 1993, **63**, 442–449.
46 X. Z. Lin, P. Liu, J. M. Yu and G. W. Yang, *J. Phys. Chem. C*, 2009, **113**, 17543–17547.
47 H. B. Hassan and Z. Abdel Hamid, *Int. J. Electrochem. Sci.*, 2011, **6**, 5741–5758.
48 M. Sanles-Sobrido, L. Rodríguez-Lorenzo, S. Lorenzo-Abalde, A. González-Fernández, M. A. Correa-Duarte, R. A. Alvarez-Puebla and L. M. Liz-Marzán, *Nanoscale*, 2009, **1**, 153–158.
49 W. Xie, P. Qiu and C. Mao, *J. Mater. Chem.*, 2011, **21**, 5190–5202.
50 M. F. Mrozek and M. J. Weaver, *Anal. Chem.*, 2002, **74**, 4069–4075.

51 X. L. Luo, J. J. Xu, W. Zhao and H. Y. Chen, *Sens. Actuators, B*, 2004, **97**, 249–255.
52 H. Wang, C. Zhou, J. Liang, H. Yu and F. Peng, *Int. J. Electrochem. Sci.*, 2008, **3**, 1180–1185.
53 H. Wang, C. Zhou, J. Liang, H. Yu and F. Peng, *Int. J. Electrochem. Sci.*, 2008, **3**, 1258–1267.
54 T. Ichimura, H. Watanabe, Y. Morita, P. Verma, S. Kawata and Y. Inouye, *J. Phys. Chem. C*, 2007, **111**, 9460–9464.
55 E. J. Blackie, E. C. Le Ru and P. G. Etchegoin, *J. Am. Chem. Soc.*, 2009, **131**, 14466–14472.
56 H. Kneipp, J. Kneipp and K. Kneipp, *Anal. Chem.*, 2006, **78**, 1363–1366.